

## MILLIMETER RADIO SPECTRO-IMAGING

P. Gratier<sup>1</sup> and J. Pety<sup>1,2</sup>

**Abstract.** In recent years, the upgrade of heterodyne spectrometers at the IRAM 30m telescope has increased the instantaneous observable bandwidth by a factor 8 with spectral resolution increase of a factor 10. We here present new results using these instrument as an example of the new challenges in data reduction and analysis in millimeter radioastronomy. In the next 5 years, wide-field, wide-bandwidth imaging or spectro-imaging will become the norm at IRAM, due to new upgrades such as the arrival of multi-beam heterodyne receivers for the IRAM 30m and a large increase of the IRAM Plateau de Bure interferometer, namely the NOEMA project. New observing and data reduction methods will have to be devised to reduce and analyze the data coming from these instruments.

Keywords: Millimeter radioastronomy, spectro-imaging

### 1 Introduction

Millimeter radio observations differ from visible observations in several aspects. Whereas in the optical domain, the atmosphere is transparent and has a brightness temperature well below that of the observed sources, the situation is reversed in the millimeter radio domain, with source brightness temperatures much smaller than atmospheric brightness temperatures (the source brightness temperatures range from a few Kelvins to tens of milliKelvins, with typical sky temperatures of 300K). Furthermore, the atmospheric transparency in the sub(millimeter) domain can be low, especially at higher frequency, and depends strongly on the water vapor content of the atmosphere. An analogy would be that radio millimeter observation are akin to observing through a fog during daylight. For these reasons, millimeter observations are almost systematically made using differential methods, subtracting from the source signal, the data from a reference position far enough from the scientific source to be devoid of its emission but close enough to sample the same atmosphere. Typical separations from source and reference are 100".

### 2 Current observing modes

Up to recently, mostly two independent approaches have typically been used in millimeter radioastronomy: either narrow band (only one to a few molecular lines) imaging or wide band (several GHz bandwidth) single pointing spectral surveys. I will use examples of real observations to illustrate these observing methods and the associated constrains on data rates and data reduction.

#### 2.1 Wide-field narrow-band imaging

##### 2.1.1 Single dish telescopes

The quantity measured at the output of a single dish telescope is the convolution of the sky brightness and the antennas point source function. This PSF is well modeled by a Gaussian of FWHM  $1.2\lambda/D$ , where  $\lambda$  is the observing wavelength and  $D$  the telescope diameter. In the case of the IRAM 30m telescope for the CO(2-1) line (1.3mm) this corresponds to 11".

---

<sup>1</sup> Institut de Radioastronomie Millimétrique, 300 rue de la Piscine, 38406 Saint Martin d'Hères, France

<sup>2</sup> LERMA, UMR 8112, CNRS and Observatoire de Paris, 61 avenue de l'Observatoire, 75014 Paris, France

To map large regions of the sky, the most recent observing technique is to slew the telescope continuously while acquiring spectra regularly spaced in time. This observing mode is known as On-The-Fly observing. The full map of the triangulum galaxy M33 in CO(1-0) with the IRAM 30m telescope (Gratier et al. 2010; Druard et al. 2012) is an example of wide field mapping (see Fig. 1). The mapped field of view is  $55' \times 40'$  ( $0.78 \text{ deg}^2$ ) with a resolution of  $12''$  this corresponds to 55 000 independent beams. The spectra are composed of 512 2 MHz wide channels for a total frequency bandwidth of 1 GHz. During the 400 telescope hours needed to complete the project,  $\sim 2 \times 10^6$  individual spectrum have be acquired with a data rate of 250 MB/hr.

### 2.1.2 Interferometric telescopes

By default, an interferometer is a mapping instrument, imaging a field of view the size of the primary beam of the antennas ( $\theta_{\text{prim}} = 1.2\lambda/D_{\text{prim}}$ ) with a resolution given by the ratio of the wavelength to the largest baseline between antennas. The area mapped by an interferometer can be increased by observing successively a mosaic of pointings separated by no more than half the primary beam size. One example of a large mosaic, is the mapping of the spiral galaxy M51 by the IRAM Plateau de Bure interferometer (Project PAWS, PI: E. Shinnerer) (see Fig. 2). This mosaic is made of 60 pointings covering a 10.5 arcminute squared region with a typical resolution of  $1''$ . This corresponds to 36 000 independent beams. The raw data rate was 180 MB/hr.

## 2.2 Single pointing wide-Band spectral surveys

The second main observing mode is wide-band spectral surveys. Instantaneous frequency coverage has increased greatly in the last couple of years. At the IRAM 30m telescope for example, the combination of EMIR receivers and Fourier Transform Spectrometers increased this number by factor 8 from 2 GHz to 32 GHz while increasing the frequency resolution by a factor 10 (from 2 MHz to 200 kHz). It has become straightforward to make complete, deep surveys of the full 1mm and 3mm bands. One such example is the Horsehead WHISPER survey (PI: J. Pety, Fig. 3) which covers the full 1, 2 and, 3mm bands (more than 130 GHz total combined bandwidth) at high spectral resolution (48 kHz at 2 and 3mm, 195 kHz at 1mm). Just at 3mm, this corresponds to 750 000 frequency channels. Usual baseline subtraction techniques consisting of windowing of individual spectral lines followed by a polynomial fitting of line free channels rapidly become inadequate when facing with spectra containing several hundred thousand channels and several hundreds to thousands spectral lines. Research is ongoing inside the GILDAS/CLASS<sup>i</sup> software to devise new methods to subtract the baselines using median filtering and wavelet decomposition.

## 3 Future instruments and observing techniques

### 3.1 Heterodyne arrays

In the near future, one way of improving the mapping sensitivity of single dish telescopes will be through the use of focal plane arrays. These are sets of independent receivers bundled together, usually in a common cryogenic assembly, in the telescope receiver cabin. IRAM is working on the development of a 25 dual-polarization beam receiver at 3mm for the 30m telescope. The beams will be distributed over a typical field of view of  $6'$  and each beam will be able to observe a 4 GHz bandwidth with a typical spectral resolution of 200 kHz.

Combined with wide band spectrometers, they will have data rates of 100 GB/hr, 40 times the current narrow band imaging rate and 6 times the current wide band imaging rate. New reduction methods will have to be devised to take into account the redundancy achieved by having several independent beams recording the same position on the sky. Roussel (2012) presents such a method applied to arrays of bolometers, particularly for the Herschel instruments.

### 3.2 On the Fly interferometry

New millimeter interferometers such as ALMA and NOEMA will have good instantaneous uv-plane coverage thanks to their large number of baselines. On-The-Fly observing methods for interferometry are being developed for these instruments. Instead of observing discrete mosaic pointings, the antennas are continuously slewed on the sky with data being regularly acquired. In the case of NOEMA, this will lead to data rates up to 625 GB/hr.

<sup>i</sup>See <http://www.iram.fr/IRAMFR/GILDAS> for more information about the GILDAS softwares.

New imaging methods (e.g. WIFSYN, Pety & Rodríguez-Fernández 2010) are developed taking into account the specificities of On-The-Fly interferometric observations.

#### 4 Conclusions

Technological developments in last years have increased dramatically the bandwidth coverage at high spectral resolution of heterodyne receivers. Today, spectral surveys with several tens of GHz of bandwidth are becoming routine observations at the 30m telescope. Future instruments (heterodyne receiver arrays for the IRAM 30m telescope and the NOEMA interferometer) will combine wide field and wide spectral bandwidth to enable spectro-imaging. With the increase in data rate and data volume new reduction and analysis tools (e.g. wavelets, redundancy, OTF interferometry imaging algorithm) will have to be developed.

#### References

- Druard, C., Braine, J., Schuster, K. F. Gratier, P., et al. 2012, A&A, in prep  
 Gratier, P., Braine, J., Rodríguez-Fernández, N. J., et al. 2010, A&A, 522, A3  
 Pety, J. & Rodríguez-Fernández, N. 2010, A&A, 517, A12  
 Roussel, H. 2012, ArXiv e-prints (1205.2576)

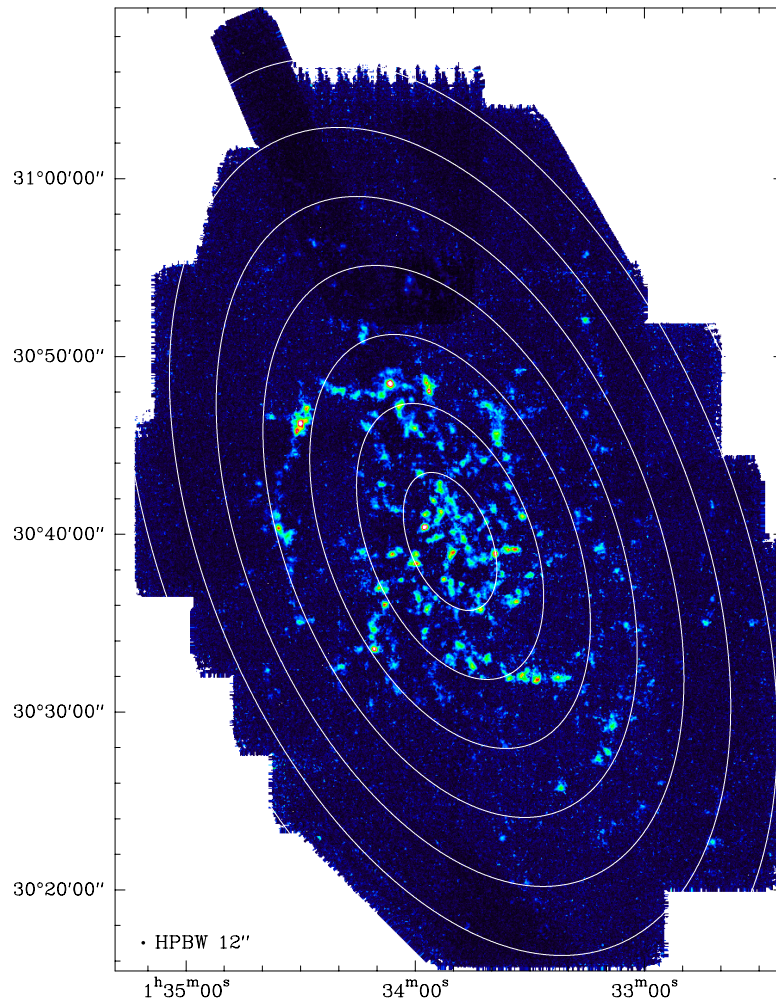


**Fig. 1.** CO(1-0) integrated intensity map of the M33 spiral galaxy observed with the IRAM 30m telescope. The resolution element is drawn at the bottom left. Ellipse are drawn every 1 kpc from the center of M33.

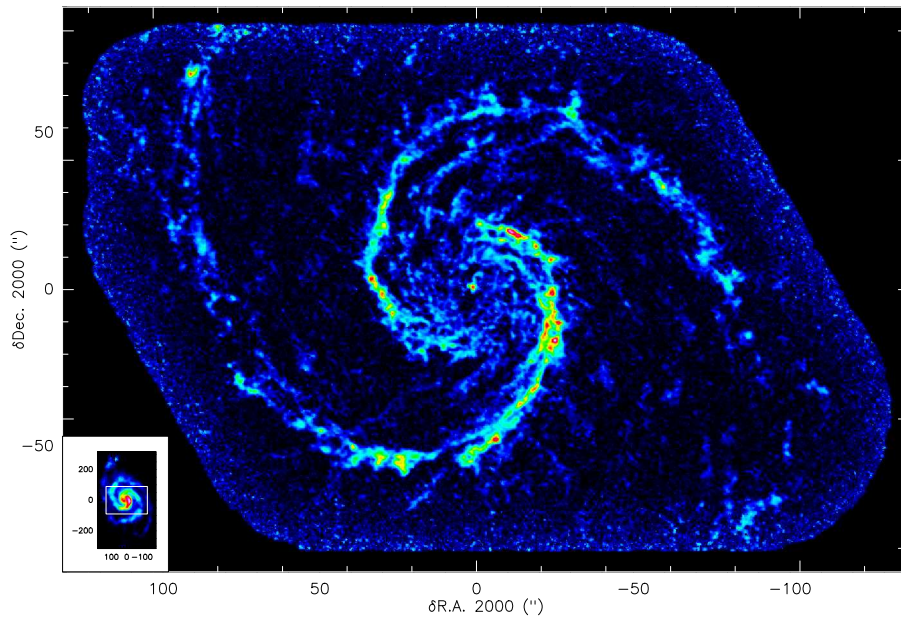


**Fig. 2.**  $^{12}\text{CO}(1-0)$  integrated emission of the inner  $\sim 10 \times 6$  kpc of NGC 5194 (aka M51a) galaxy. The coordinate offsets are relative to the nucleus of NGC 5194. This image results from the joint deconvolution of the IRAM-30m single-dish and Plateau de Bure interferometer data sets. The image inserted at the bottom left is the  $^{12}\text{CO}(1-0)$  integrated emission of the full M51 system (i.e., NGC 5194 + NGC 5195) as observed by the IRAM-30m telescope. The white horizontal rectangle shows the PAWS field of view. The images were scaled so that the angular resolution of both data set occupies the same size on the paper. In other words, the PAWS image shows the center of the small image zoomed by a factor 21.

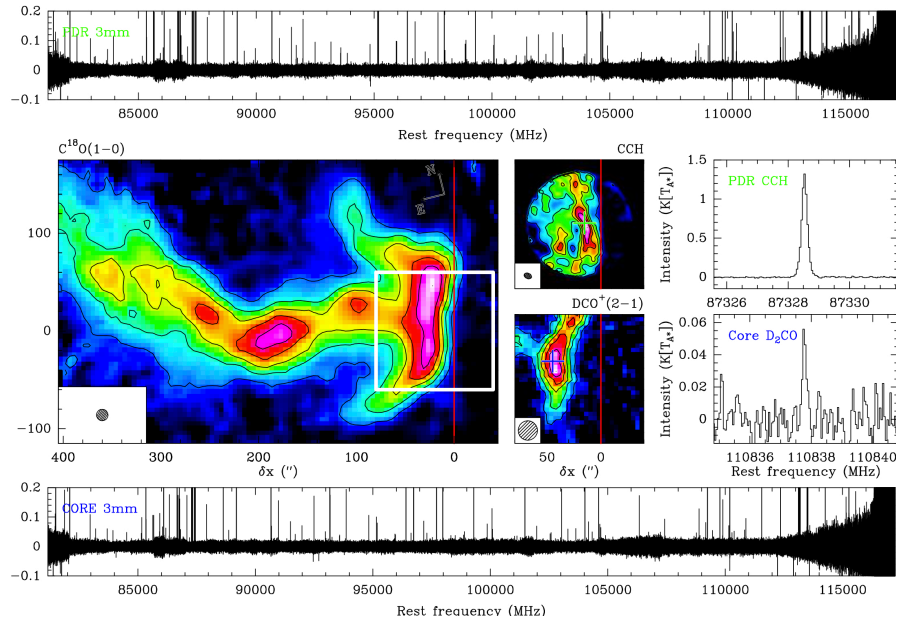


**Fig. 3.** The upper and lower panels display the spectra of the 3mm band at a spectral resolution of 49 kHz for two different positions in the Horsehead Nebula, obtained at the IRAM-30m with the combination of EMIR receivers and FTS backends in about 60 hours. Each spectra has 750 000 channels, as much information as in an image of  $860 \times 860$  pixels! The median noise is about 8 mK [Ta\*]. The survey positions correspond to two different environment located inside the white square on the  $\text{C}^{18}\text{O}(1-0)$  integrated emission map (wide, left image): 1) the photo-dissociation region (PDR) marked by the green cross on the CCH emission map (middle, top image from IRAM/PdBI), and 2) the dense core marked by the blue cross on the  $\text{DCO}^+$  emission map (middle, bottom image from IRAM/PdBI). The middle right panels display two lines zoomed from the line surveys.